Rev. Adv. Mater. Sci. 51 (2017) 16-34

RESEARCH PROGRESS IN STRENGTHENING SURFACE PERFORMANCE OF IRON AND STEEL MATERIALS BY DOUBLE GLOW PLASMA SURFACE ALLOYING TECHNOLOGY: A BRIEF REVIEW

Naiming Lin[1,2,3], Qiang Liu[1], Ruizhen Xie[1], Jiaojuan Zou[1], Dali Li[1], Shuo Yuan[1], Zhenxia Wang[1], Yong Ma[1], Xiaoping Liu[1], Zhihua Wang[2] and Bin Tang[1]

[1]Research Institute of Surface Engineering, Taiyuan University of Technology, Taiyuan, 030024, P. R. China
[2]Shanxi Key Laboratory of Material Strength and Structure Impact, Taiyuan University of Technology, Taiyuan, 030024, P R China
[3]Department of Chemical and Materials Engineering, University of Alberta, Edmonton, AB T6G 1H9, Canada

Received: February 22, 2017

Abstract. Due to their advantages of abundant resources, low cost, easy workability, stable quality and promising comprehensive mechanical properties, iron and steel materials have been widely used in various engineering fields. However, friction and wear, corrosion which usually occur on the surfaces of iron and steel components can lead to degradations in both properties and performance on their surfaces, and then may result in completely failures of the entire components. Surface treatment technologies have long been applied to improve the service performance of iron and steel materials with great success. Double glow plasma surface alloying (DGPSA) which was inspired by accidental phenomena during the plasma nitriding trials of iron and steel materials in 1980s, has been confirmed as an effective approach to provide satisfactory surface protection and strengthening of metallic materials. DGPSA can realize surface alloying by both non-metallic elements and solid metallic elements as alloying elements to create a strong/gradient metallurgical bonding between the alloyed surface and the substrate. This review began with a brief introduction of DGPSA. The research progress in strengthening surface performance of iron and steel materials by DGPSA process were reviewed and summarized in the sight of various acquired properties.

1. INTRODUCTION

Owing to their abundant in natural resources and also holding several promising merits of low cost, easy for processing, stable quality and high comprehensive mechanical properties, iron and steel materials have been widely applied in an extensive range of engineering fields, such as metallurgy, mining, machinery, architecture, chemistry, transportation and marine [1]. However, iron and steels are prone to deactivation when they are exposed to the complex and adverse working conditions, and the main damage types in application are wear and corrosion [2]. The mentioned types of material degradation usually generate on the surface of a component. Surface modification technologies allow the realization of a favorable compromise between cost and performance by endowing the material surface with high hardness value, effective friction-reduction, improved wear resistance, excellent corrosion resistance and promising mechanical performance, without affecting the entire structure of the material [3]. Double glow plasma surface alloying technology (referred to as DGPSA in the following) which was developed based on the plasma nitriding and

Corresponding author: Naiming Lin e-mail: lnmlz33@126.com

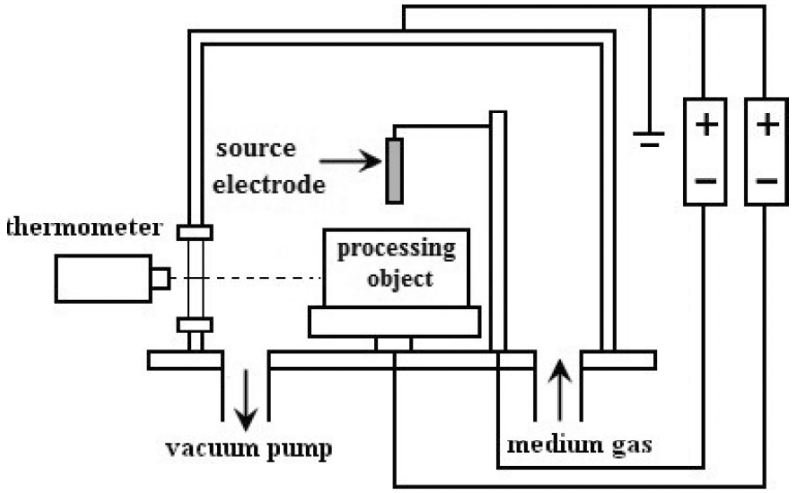

Fig. 1. Schematic diagram of DGPSA apparatus. reprinted with permission from N.M. Lin, H.Y. Zhang, J.J. Zou and B. Tang // Rev. Adv. Mater. Sci. 38 (2014) 61 and N.M. Lin, J.J. Zou, M.L. Li, J.W. Guo, Y. Ma, Z.X. Wang, Z.H. Wang, X.P. Liu and B. Tang // Rev. Adv. Mater. Sci. 44 (2016) 238. (c) 2014 and 2016 Advanced Study Center Co., Ltd.

sputtering techniques more than 30 years ago is able to accomplish surface alloying by both non-metallic elements and solid metallic elements as alloying elements [4–14]. DGPSA was invented by Professor Zhong Xu in 1980s [4–14], which had been successively covered by US and other international patents at that time. In this review, the technological principle of DGPSA was briefly introduced at first, and the research progress in strengthening surface performance of iron and steel materials by DGPSA process were presented and summarized in the sight of various acquired properties. This work is expected to create database and provide reference information, thereby furtherly broaden the practical applications of DGPSA on iron and steel materials.

2. PRINCIPLE AND PROCESSING RESEARCH OF DGPSA PROCESS

2.1. Principle of DGPSA

The DGPSA was evolved on the basis of plasma nitriding and sputtering techniques, hence a chamber equipped with a complete vacuum system is necessary. Fig. 1 presents the schematic diagram of DGPSA apparatus. The technological principle of DGPSA had already been systemically introduced in our published reviews [4,7]. However, the present article can also be considered as a relatively independent part belonging to the applications of DGPSA, therefore the principle of DGPSA has been briefly introduced here all the same. In the vacuum chamber, the processing object (work piece) and the so called source electrode (removable target made up of one or more desired alloying elements) are two negatively charged units and the earthed vacuum bell jar is the anode. As shown in Fig. 1, as the two power supplies were turned on and reached certain voltage values, both processing object and source electrode would be enveloped in glow discharge under the argon plasma atmosphere. One glow discharge can bring about activation and heating on the surface of processing object to make contributions to surface alloying. While the other glow discharge bombards the source electrode to sputtering out the desired alloying elements. This phenomenon was discovered during the process studies on plasma nitriding of steel and was named as “double glow discharge” by Professor Zhong Xu. DGPSA was covered by US patent in 1985. More importantly, DGPSA was the very first granted US patent since the founding of the People’s Republic of China, and then it was successively authorized as patents in different countries [4–7].

The charged ions or particles which are bombarded from the source electrode transport to processing object and firstly diffuse into then deposit onto the surface of the processing object under the influence of an electric field, and finally receiving an alloyed surface. The thickness values of the surface alloying layers vary from several micrometers even to 500 μm, with alloying elements in a gradient concentration of a few percent to 90% or more [4–7].

There are two modes to achieve surface alloy via DGPSA which can improve the surface perform-

ance of iron and steel materials in different degree. One is single element alloying by DGPSA, alloying with single non-metallic elements (NME) and solid metallic elements (ME); the other is binary element alloying by DGPSA, existing NME + NME, NME + ME and ME + ME. The NMEs contain boron (B), carbon (C), and nitrogen (N), while the MEs cover a series of elements: aluminum (Al), chromium (Cr), Copper (Cu), molybdenum (Mo), niobium (Nb), nickel (Ni), tungsten (W), and zirconium (Zr). Also minor studies on multi-alloying by the collocation of ME and NME have been conducted [4,7]. The positive roles of the mentioned elements lie in the following aspects: formation of hard phases in the coating or in the near surfaces, obtaining excellent corrosion resistance by receiving passive or chemical stable coating/layer on the surfaces of iron and steel materials.

DGPSA possesses a series of merits, several most important features are listed as follows [4–7]: (1) resource and precious metal element conservation, (2) free of pollution (In most cases, argon (Ar) gas was chosen as the carrier gas), (3) controlled alloying composition on the surface, (4) wide range selection of alloying elements, (5) gradient distributions of the composition, structure and property, (6) holding a metallurgical bond between alloyed layer and substrate. Since the double glow discharge phenomenon was discovered, great deals of studies on DGPSA processing were firstly conducted to improve the surface performance of iron and steel materials.

2.2. Processing research of DGPSA

As mentioned above, DGPSA was accidentally discovered by Professor Zhong Xu during the process studies on plasma nitriding of steels, therefore most processing studies of DGPSA were mainly concentrated on iron and steel materials in the early period. Because of the alloying process of DGPSA was still controlled by diffusion, so temperature and soaking time were the main determined parameters which can affect the thickness of the obtained alloyed layer. Processing parameters of bias voltage of processing object, bias voltage of source electrode and gas pressure had certain effects on alloying temperature. Higher bias voltage definitely resulted in higher alloying temperature. However it was obviously not that higher temperature could form better alloying coating. In respect of processing object, the alloying temperature should not be too high to weaken the entire mechanical property of work piece as a precondition. Temperature on its surface was controlled by stepping the voltages of processing object and source electrode up or down. With respect to source electrode, in order to improve the amount of sputtering, bias voltage of source electrode was regulated to reach a temperature just below the melting point of source electrode based on specific cases. Meanwhile a much higher bias voltage of processing object which might lead to re-sputtering of the alloying element on the processing object surface originally from the source electrode, also had side effect on alloying process. Additionally, an optimal voltage difference between the processing object and the source electrode could maintain constant glow discharge in the chamber. A proper gas pressure in the vacuum furnace was helpful to achieve steady discharge and generated uniform plasma. On the other hand, source electrode shape and distance between the processing object and the source electrode could also influence the alloying process. Plate source electrode with different compositions as needed was the most used shape by easy manufacturing, also some special shapes of source electrodes were developed to realize surface alloying of processing object with different geometric shapes and improve the sputtering rate. A proper distance between the processing object and the source electrode was able to benefit the alloying process. A long distance meant the sputtered element would transport through a long distance, scattering of moving atoms was inevitable, and this could result in lower utilization of sputtered element. While a short distance was prone to induce arc discharge, which was going to burn-out both processing object and the source electrode [4,7]. These processing parameters were not the same, in most situations they varied and were case-by-case. Some typical examples of DGPSA on iron and steel materials were listed as follows.

He et al. [8] conducted W-DGPSA and Ni-Cr-DGPSA on cast irons using plate source electrodes. It was found that the diffusion coefficients of alloying elements revealed exponential relation to temperature, while the relationship between thickness value and soaking time followed parabolic functions. It meant that alloying temperature played more significant effect on thickness of alloyed coating than soaking time. The proper parameters of DGPSA on cast irons were: bias voltages of source electrode -800~-1000 V, bias voltages of processing object -300~-500 V, gas pressure values 30~50 Pa, distances between the processing object and the source electrode 15~20 mm.

Wang et al. [9] investigated the simplification of processing research to favor practical application.

The results showed that when the source electrode and the processing object were with similar areas, constant and stable discharge appeared on the source electrode and the processing object would obtain a uniform alloyed surface.

Tang et al. [10] realized several chromizing processes on Q235 steels via DGPSA under a bias voltage of source electrode -1000 V, bias voltages of processing object -300~-480 V, gas pressure 30 Pa, distances between the processing object and the source electrode 35 mm. The obtained chromizing coatings varied in thickness value and structure characterization (single deposition/diffusion layer or deposition + diffusion layer).

The multi-element Ni-Cr-Mo-Nb surface alloying on pure iron was conducted by Zhang et al. [11] by DGPSA using an Inconel 625 alloy source electrode. It was found that the DGPSA indicated a diffusion coefficient of ~10^{-8} m^2/s which was higher than the diffusion coefficient of common surface alloying process. Meanwhile Ni and Cr revealed higher diffusion coefficients in comparison to Mo and Nb, which were closely related to their atomic radius sizes.

Cooling rate which played an important role in the formation of precipitates during cooling process, had significantly effect on the structure and performance of the alloying coating. Zhao et al. [12] drew a Time-Temperature-Transformation (TTT) diagram of W-Mo-DGPSA treated 20 steel. It was found that when the cooling process was just furnace cooling, topo-logically closed (TCP) phase precipitated during this process. TCP phase was a detrimental phase, it could result in heterogeneous distribution of elements in the alloying coating and then weaken the performance of the alloying coating. When the DGPSA was done, a cooling rate of 60 °C/min was applied for 6 min and then cooling slowly could effectively reduce detrimental precipitate.

Gu et al. [13] prepared the Fe-Al intermetallic modified layer on 45 steel by DGPSA. The coating was metallurgically bonded to the substrate, and its overall thickness was nearly 10 μm. The modified layer consisted of a deposition layer and a diffusion layer, and mainly contained FeAl, Fe_3Al, and α-Fe (Al) phases. The elemental composition presented gradient distribution. And it performed good combination between the modified layer and the matrix.

Bu et al. [14] carried out titanizing on low-carbon steel by pulse power glow plasma and studied the distribution of alloying elements and the thickness of Ti layer with voltage, time and temperature at different levels. The thickness of titanized layer was more than 200 μm and had a distinct reaction-diffusion line between the layer and the substrate. The titanized layer was composed of Fe_2Ti, Fe-Ti and TiC. With increasing the voltage, the layer became thicker, and the thickest was achieved at 550 V. However, when the voltage exceeded 550 V, the thickness and Ti content of the layer was decreased. With prolonging the time, the thickness and Ti content of the layer was increased. While under higher temperature, the thickness the Ti content of the layer was increased, too.

Wang et al. [15] analyzed the primary process parameters and its effects on industrial manufacture of DGPSA. The results showed that discharge power of the source surface was the primary process parameter of effects on the alloying layer. As the alloy element layer was needed to produce cathode sputtering from the source, so the double glow plasma surface alloying process must maintain sufficient discharge power for the source. Its size was directly proportional to the depth of the layer and the concentration of the surface alloy.

Li et al. [16] obtained dense alumina coating by the oxidation of Al layer prepared by the DGPSA. The quality, thickness and Al content of Al coating were affected by the process parameters. The optimum technological parameters were: pressure 35 Pa, source voltage -850 V, workpiece pole voltage -300 V, pole spacing 15 mm, time 3 h. The maximum thickness reached 31.70 μm. After the thermal oxidation of the Al layer, the coating with a thickness of 10 μm Al_2O_3 was obtained.

Ren et al. [17] formed surface age-hardening alloy of Fe-W-Mo-Co on surface of low-alloyed steel by DGPSA. The results suggested that technological parameters had effect on thickness of the layer and distribution of composition. The contents of W, Mo, Co in the layer, under parameters: V_s, 950 V; I_s, 1.0 A; V_A, 550 V; I_A, 4.2 A, nearly reached the content level of age-hardening alloy W11Mo7Co23 (Fig. 2).

Wang et al. [18] studied the effects of process parameters on the phase structure of TiN layer by DGPSA. When the TiN layer thickness was low, the growth of TiN layer presents {100} oriented growth trend under the control of surface energy, so that the free energy was lower in TiN layer system; When the TiN layer was thicker, the strain energy was the dominant factor, it played a major control action in the growth of TiN layers, so that TiN layer presenting {111} preferred orientation, that was conducive to TiN layer of the system free energy reduction. With the increasing in the thickness of the TiN layer, {111} preferred orientation growth was more significant.

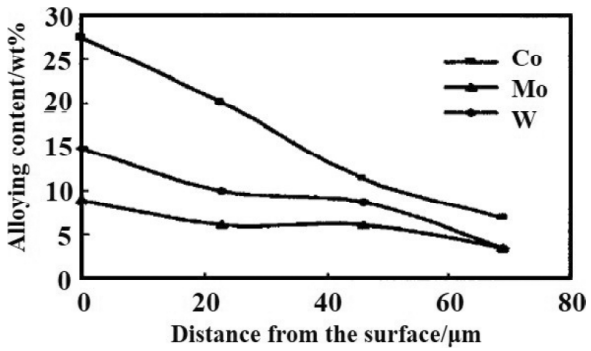

Fig. 2. Distribution of alloying elements along the percolation layer. reprinted with permission from N.J. Ren, W.Q. Wang, Y.M. Zhang, Z.H. Li and Z. Xu // J. Taiyuan Univer. Technol. 34 (2003) 261. (c) 2003 Journal of Taiyuan University of Technology Editorial Office.

3. ACQUIRED PROPERTIES ON STEELS BY DGPSA

3.1. Wear resistance

Zhou et al. [19] prepared Nb layers on 45 steel surface using DGPSA to improve its wear resistance. The concentration of Nb decreased gradually along the depth of alloyed layer which contributed a metallurgical bonding with the matrix. The thickness of Nb layer was approximately 10 μm, it was composed of Nb, Fe_2Nb, NbC, and Nb_2C. The concentration of Nb gradually decreased along the depth of alloyed layer which confirmed a metallurgical bonding with the matrix. The surface hardness of was 2-3 times higher than the substrate. The ball-on-disc wearing tests indicated that the friction co-efficient decreased from 0.80 to 0.15 and the worn mass was only 18% of that of the matrix at room temperature.

Qiu et al. [20] prepared a dense W-Mo coating on 16Cr3NiWMoVNbE gear steel by employ of DGPSA technique. The hardness, elasticity modulus, scratch test and tribological behavior of the W-Mo coating were both measured. The coating was metallurgically bonded to the substrate without defects of pores or cracks and its overall thickness was nearly 12.5 μm. The coating was composed of deposition layer and diffusion layer. The thickness of the deposition layer was about 10 μm, consisting of W and Mo elements. Diffusion layer was beneath the deposition layer and its thickness was about 2.5 μm. The diffusion layer consisted of Fe from the substrate diffused into the coating and W-Mo from coating diffused into the substrate. The EDS analysis revealed that W, Mo, and Fe existed in a gradient distribution in the diffusion layer. The existence of the diffusion layer between the coating and the substrate formed a transition zone which was beneficial to the interfacial bonding strength of the coating. In terms of H/E and H_3/E_2 ratios, the coated sample was nearly 2 times better than that of the uncoated sample, which reflected a good plastic deformation resistance. The obtained coating presented promising bonding strength to the substrate. The W-Mo coating indicated lower friction coefficient than those of uncoated samples at room and 500 °C high temperature, and the specific wear rates of the W-Mo coating at room and 500 °C high temperature were 8.1×10^{-5} $mm^3\cdot N^{-1}\cdot m^{-1}$ and 11.2×10^{-5} $mm^3\cdot N^{-1}\cdot m^{-1}$ respectively, which were about only 19% of the uncoated samples. Furthermore, the wear mechanism of the W-Mo coating was mainly abrasive wear at room temperature and oxidative wear at high temperature. The excellent wear resistance of the W-Mo coating might be due to its high resistance to plastic deformation and load bearing capacity.

Zhang et al. [21] prepared Cu modified layer on the surface of AISI304 stainless steel by DGPSA. The modified layer composed of a mixture of Cu and expanded austenite phase was a duplex layer (deposited + diffused layer) with thickness of about 26 μm under the optimum process parameters. The ball-on-disk results showed that the modified layer possessed low friction coefficient of about 0.25 and excellent wear resistance.

Zhang et al. [22] obtained a Cu modified layer on AISI304 stainless steel using DGPSA and wear behavior of the modified layer sliding against different counterparts was investigated using a ball-on-disc tester in ambient air. The results showed that the surface modified layer with the thickness of about 26 μm was uniform and dense (Fig. 3), which was mainly composed of pure Cu, expanded austenite phase and a few Fe_3O_4 phase. The Cu modified layer significantly improved the tribological properties of stainless steel as sliding against GCr15, while higher wear rate and friction coefficient were obtained for sliding friction of the modified layer against Al_2O_3 (Fig. 4).

Gao et al. [23] formed high chrome layer on cheaper low carbon steel surface by DGPSA. The surface composition was more than 40%. Afterward plasma carburizing was processed on alloyed high chromium layer. The carbonization layer was dispersion, thin and uniformity. The content of carbon on the surface was more than 2.8%. The surface hardness was 1800 HV after quenching and tempering. The wear resistant was 8 times higher than that of GCr15 steel.

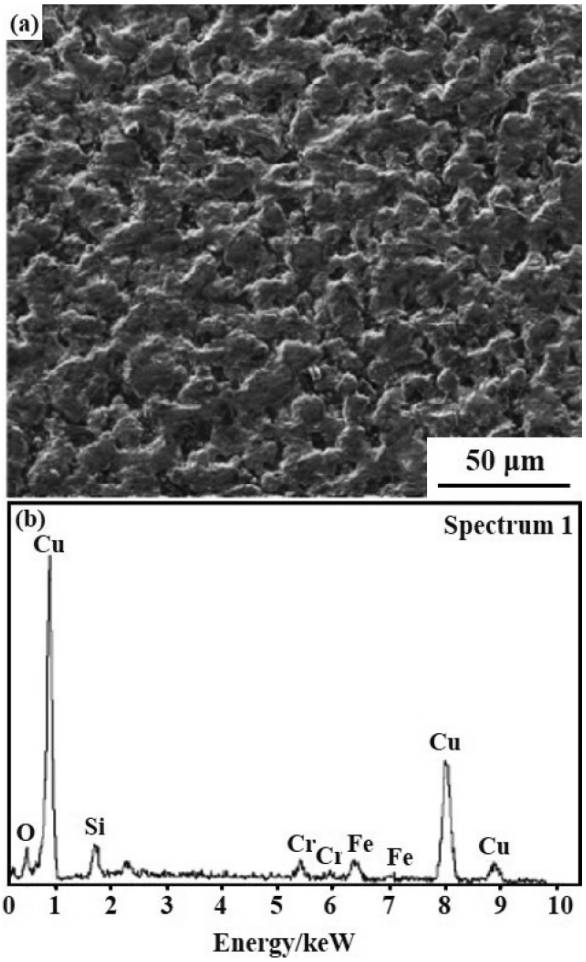

Fig. 3. SEM micrograph of the Cu modified stainless steel and corresponding EDS spectrum. reprinted with permission from X.Y. Zhang, B. Tang, A.L. Fan, R.H. Zhu and H.F. Wang // Trans. Mater. Heat Treat. 32 (2011) 136. (c) 2011 Transactions of Materials Heat Treatment Editorial Office.

Shen et al. [24] prepared Zr/ZrC gradient alloying layer by DGPSA to enhance the surface hardness and wear resistance of AISI 440B stainless steel. The alloying surface consisted of Zr-top layer and ZrC-subsurface layer which was strongly bonded to the AISI 440B steel substrate. The thickness of the Zr/ZrC alloying layer gradually increased from 16 μm to 23 μm with alloying temperature elevated from 900 °C to 1000 °C. With alloying time from 0.5 h to 4 h, the alloyed depth increased from 3 μm to 30 μm, and the ZrC-rich alloyed thickness vs. time was basically parabola at temperature of 1000 °C. Both the hardness and wear resistance of the Zr/ZrC alloying layer were obviously improved as compared with the untreated AISI 440B steel.

Wu et al. [25] fabricated Cu alloyed layer on the stainless steel for solve the problems of poor forming and weak adhesion by DGPSA. The analyses for microstructure and incremental forming were conducted. The Cu alloyed layer formed a solid solution at certain temperature. The supersaturated Cu crystal grain in Fe will dispersedly precipitated in grain interior and crystal boundaries and form the vermicular structure. The typical XRD patterns revealed that Cu alloyed layer was mainly composed of Fe-Cu alloy phase with a high hardness and an enhanced thermal stability. It was confirmed that Cu alloyed layer with a cubic crystal structure were more easily deformable than that of stainless steel. The tribological tests revealed that the frictional coefficient of the Cu alloyed layer gradually decreased as the time increased, while the stainless steel showed an increase in the frictional coefficient. The wear rate of the Cu alloyed layer was approximately 2 times lower than that of the stainless steel. Re-

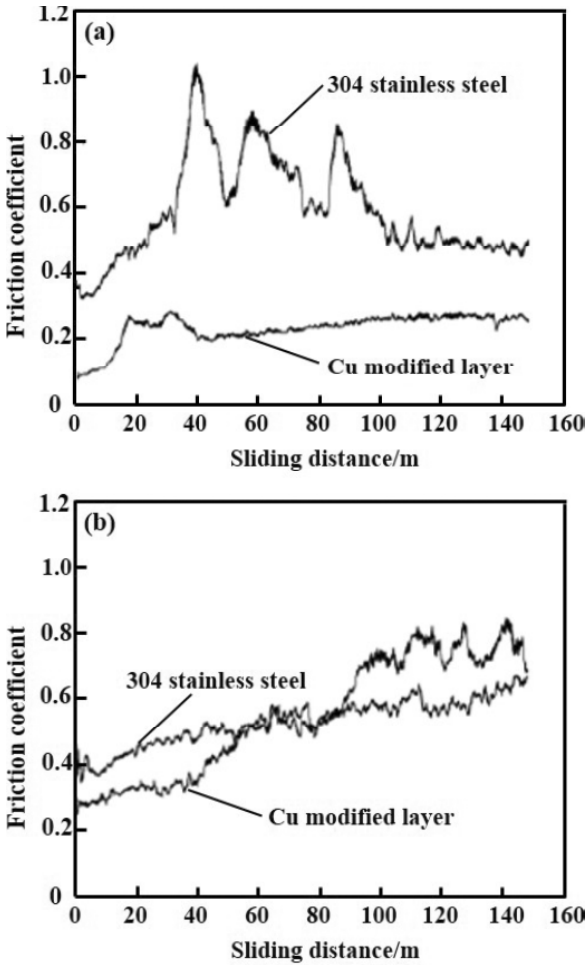

Fig. 4. Curves of friction coefficient vs. sliding distance for untreated and treated samples tested against (a) GCr15 and (b) Al_2O_3. reprinted with permission from X.Y. Zhang, B. Tang, A.L. Fan, R.H. Zhu and H.F. Wang // Trans. Mater. Heat Treat. 32 (2011) 136. (c) 2011 Transactions of Materials Heat Treatment Editorial Office.

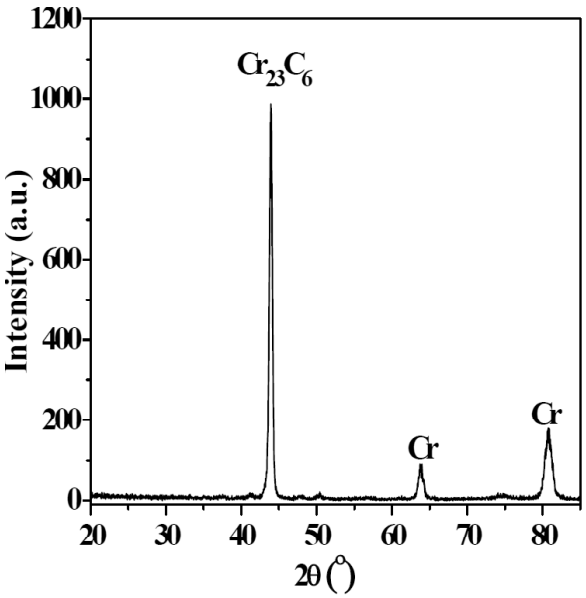

Fig. 5. XRD pattern of chromizing coating. reprinted with permission from N.M. Lin, P. Zhou, H.W. Zhou, J.W. Guo, J.J. Zou, W. Tian, X.F. Yao and B. Tang // Kovove Mater. 53 (2015) 147. (c) 2015 Institute of Materials and Machine Mechanics, Slovak Academy of Sciences, Bratislava, Slovak Republic.

sults of the incremental forming indicated that Cu alloyed layer and the stainless steel embodied the similar buckling failure to a certain extent. Cu alloyed layer reduced the surface ploughing effect. On the contrary, the stainless steel exhibited an obvious ploughing damage.

Lin et al. [26] employed DGPSA to carry out chromizing of P110 oil casing tube steel aim to improve its surface performance. Electrochemical experiments, including open circuit potential (OCP) and potentiodynamic polarization were conducted in CO_2 saturated simulated oilfield brine to assess the corrosion resistance of the chromizing coating. According to the diffraction peak intensity (Fig. 5), it can be identified that the obtained coating mainly composed of $Cr_{23}C_6$, and this indicates the formation of chromizing coating. It was seen that besides the $Cr_{23}C_6$, weak Cr peaks advent in the XRD pattern and this might be resulted from the formation of a Cr-Fe solid solution in the chromizing coating. It was revealed that chromizing coating was uniform and compact (Fig. 6) without any micro-cracks. The microstructure of the chromizing coating on P110 steel was analyzed under an OM on transverse nital-etched micro-section. A bright, non-etched layer with an estimated thickness of 35 ìm was observed according to the measuring scale, the obtained coating was dense, uniform and compact and it was clearly separated from the P110 steel substrate (Fig. 7a). GDOES compositional depth profile was presented in Fig. 7b, it was seen that the concentration of Cr gradually decreased from outside to inside, and the concentration of Fe increased from the surface to interior. While the gradient distributing characteristics of Cr and Fe in the coating were conducive to improve the bond strength between the coating and the substrate. The thickness of the chromizing coating was approximately 35 ìm, as derived from GDOES analysis, and that was in good agreement with the OM observation. The chromizing coating with higher surface hardness (Fig. 8) showed better wear resistance than that of P110 steel indicating by lower mass losses and narrower wear trace (Fig. 9 and Fig. 10). The chromizing coating also exhibited higher open circuit potential and lower corrosion current density in comparison to P110 steel (Fig. 11 and Fig. 12). Plasma surface chromizing was considered as a potentially effective method for improving the wear and corrosion resistance of P110 steel.

Zheng et al. [27] studied the chromizing hardening process of carbon tool steel by using double glow plasma surface chromizing process and plasma nitriding at 560 °C. The results showed that the obtained layer consisted of deposition layer and diffusion layer. The depth of deposition layer was 4~5 μm and the content of chromium was more than

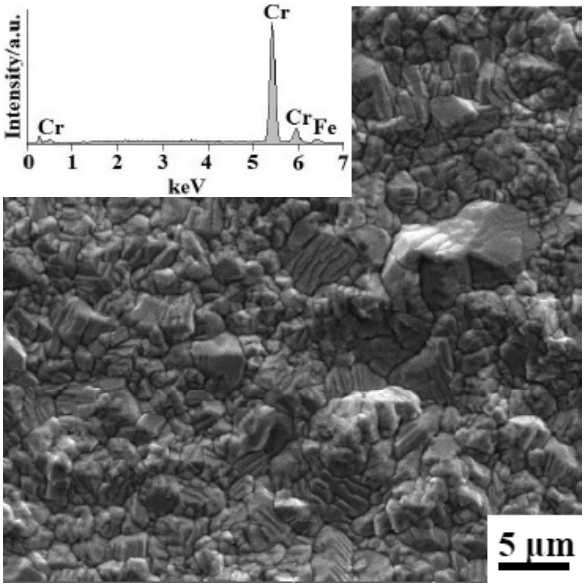

Fig. 6. Surface morphology of chromizing coating. reprinted with permission from N.M. Lin, P. Zhou, H.W. Zhou, J.W. Guo, J.J. Zou, W. Tian, X.F. Yao and B. Tang // Kovove Mater. 53 (2015) 147. (c) 2015 Institute of Materials and Machine Mechanics, Slovak Academy of Sciences, Bratislava, Slovak Republic.

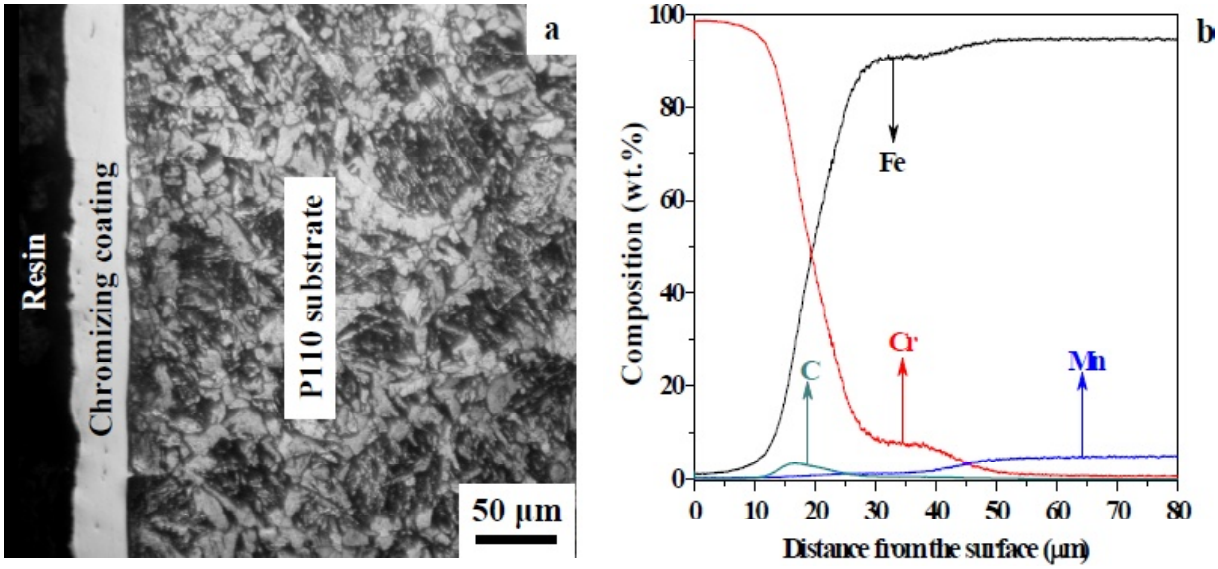

Fig. 7. Cross-sectional microstructure (a) and composition profile of chromizing coating (b). reprinted with permission from N.M. Lin, P. Zhou, H.W. Zhou, J.W. Guo, J.J. Zou, W. Tian, X.F. Yao and B. Tang // Kovove Mater. 53 (2015) 147. (c) 2015 Institute of Materials and Machine Mechanics, Slovak Academy of Sciences, Bratislava, Slovak Republic.

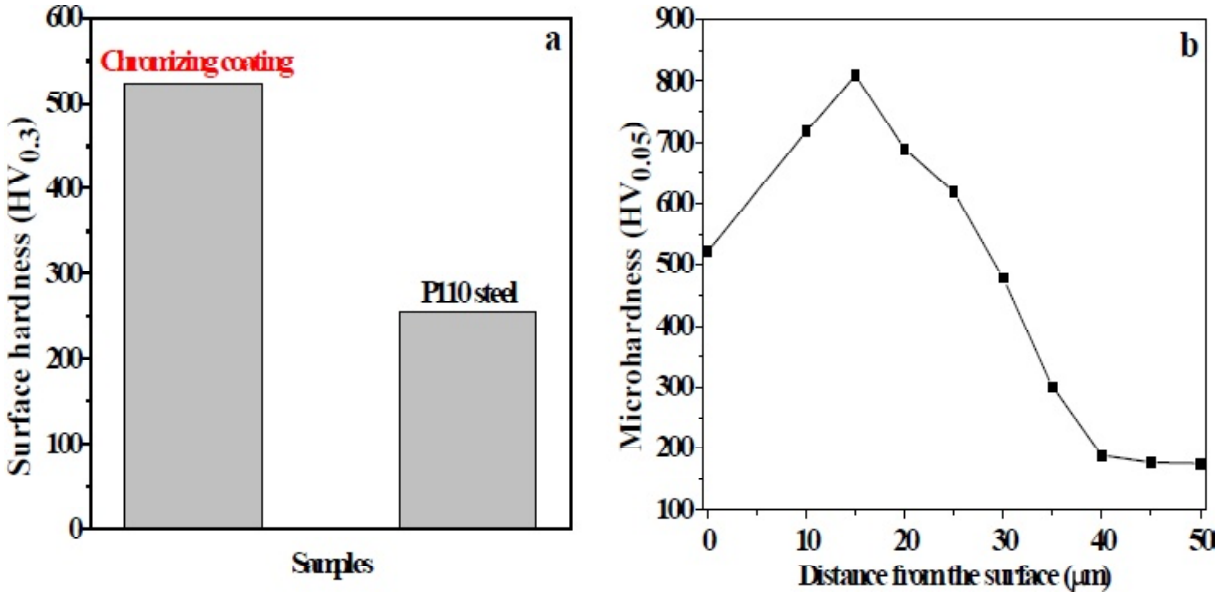

Fig. 8. Surface microhardness values of chromizing coating and P110 steel (a) and microhardness profile of chromizing coating. reprinted with permission from N.M. Lin, P. Zhou, H.W. Zhou, J.W. Guo, J.J. Zou, W. Tian, X.F. Yao and B. Tang // Kovove Mater. 53 (2015) 147. (c) 2015 Institute of Materials and Machine Mechanics, Slovak Academy of Sciences, Bratislava, Slovak Republic.

50%, which was closely bonded to the substrate. The chromium distribution of diffused layer was in gradient and the depth was 20~25 μm. The phase composition of alloyed layer consisted of Fe-Cr, CrN, Cr_7C_3, and $Cr_{23}C_6$. The hardness of chromized layer was more than 1000 HV and distribution of hardness was in gradient, which had not changed the structure and property of the substrate material.

Chi et al. [28] studied chromizing process of T8 steel via DGPSA. The results showed that a good chromized layer could be also gained in T8 steel by low temperature double glow plasma chromizing process. The layer consisted of deposition layer, carbide layer and solid solution layer. After 3 h treatment, the thickness of the chromized layer reached to 80 μm, the highest hardness was about 1400 HV (Fig. 13).

Liu et al. [29] formed a Mo alloying layer on the surface of 304 stainless steel using DGPSA to improve the wear resistance performance of 304 stain-

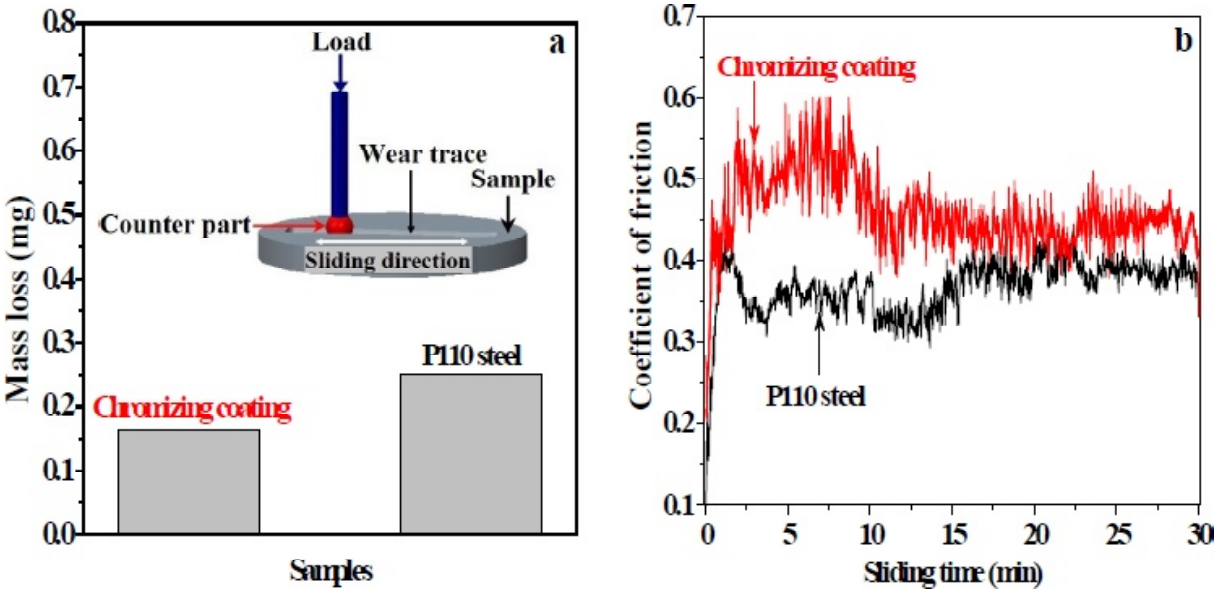

Fig. 9. Mass losses (a) and coefficients of friction (b) of chromizing coating and P110 steel. reprinted with permission from N.M. Lin, P. Zhou, H.W. Zhou, J.W. Guo, J.J. Zou, W. Tian, X.F. Yao and B. Tang // Kovove Mater. 53 (2015) 147. (c) 2015 Institute of Materials and Machine Mechanics, Slovak Academy of Sciences, Bratislava, Slovak Republic.

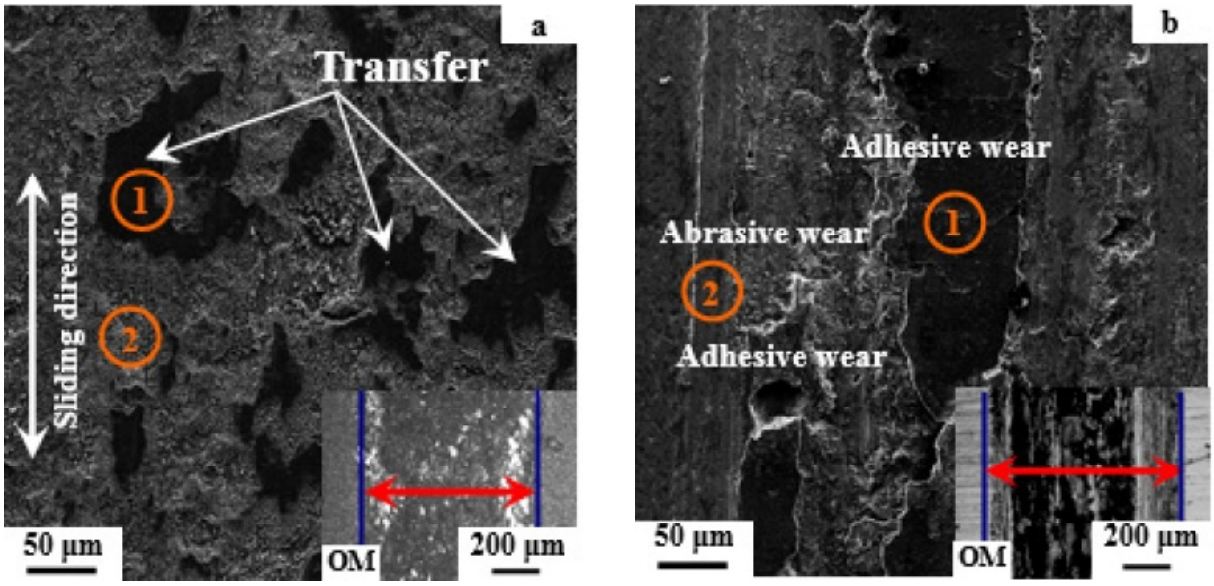

Fig. 10. Wear scars of chromizing coating (a) and P110 steel (b). reprinted with permission from N.M. Lin, P. Zhou, H.W. Zhou, J.W. Guo, J.J. Zou, W. Tian, X.F. Yao and B. Tang // Kovove Mater. 53 (2015) 147. (c) 2015 Institute of Materials and Machine Mechanics, Slovak Academy of Sciences, Bratislava, Slovak Republic.

less steel. The prepared Mo alloying layer was homogeneous and compact, and the thickness was about 9.6 μm (Fig. 14). The layer mainly consisted of Mo, and the Mo element in the alloying layer showed a gradient distribution from the surface to the beneath substrate. The average surface microhardness value was about 806 $HV_{0.05}$. Under dry friction conditions, the wear rate of 304 stainless substrate was about 84 times higher than that of the Mo alloying layer, leading to significantly improved wear resistance (Fig. 15).

Liu et al. [30] modified stainless steel substrate at 600 °C via DGPSA to form Al_2O_3 ceramic coatings. The results showed that the phases and microstructure of Al_2O_3 coatings were strongly influenced by the oxygen flow rate. The dense and smooth Al_2O_3 coatings were successfully prepared at the oxygen flow rate of 15 sccm. The significant influ-

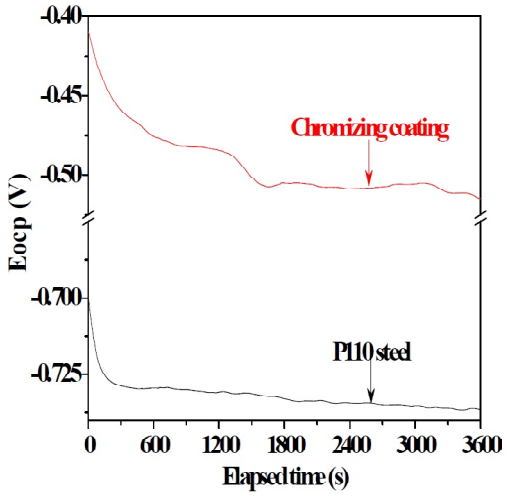

Fig. 11. Eocp vs. time curves of chromizing coating and P110 steel. reprinted with permission from N.M. Lin, P. Zhou, H.W. Zhou, J.W. Guo, J.J. Zou, W. Tian, X.F. Yao and B. Tang // Kovove Mater. 53 (2015) 147. (c) 2015 Institute of Materials and Machine Mechanics, Slovak Academy of Sciences, Bratislava, Slovak Republic.

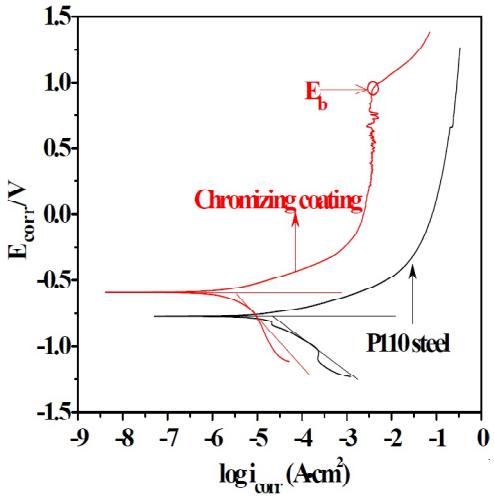

Fig. 12. Polarization curves of chromizing coating and P110 steel. reprinted with permission from N.M. Lin, P. Zhou, H.W. Zhou, J.W. Guo, J.J. Zou, W. Tian, X.F. Yao and B. Tang // Kovove Mater. 53 (2015) 147. (c) 2015 Institute of Materials and Machine Mechanics, Slovak Academy of Sciences, Bratislava, Slovak Republic.

ence of the oxygen flow on the mechanical properties of Al_2O_3 coatings was also confirmed. The results were in good agreement with the microstructural analysis. A maximum hardness of 31 GPa and elastic modulus of 321 GPa were obtained at the oxygen flow rate of 15 sccm. At the same time, coatings obtained at a 15 sccm oxygen flow rate showed the best adhesion strength of 47 N.

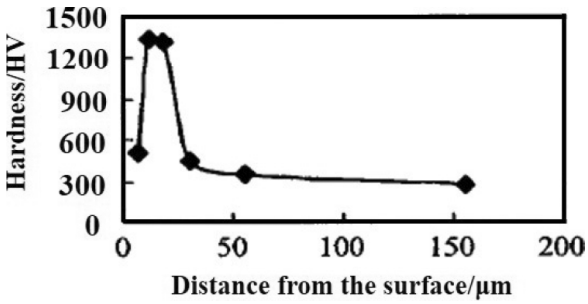

Fig. 13. Microhardness distribution of modified layer. reprinted with permission from C.Z. Chi, Y. Gao, J.X. Zhao and Z. Xu // J. Taiyuan Univer. Technol. 34 (2003) 285. (c) 2003 Journal of Taiyuan University of Technology Editorial Office.

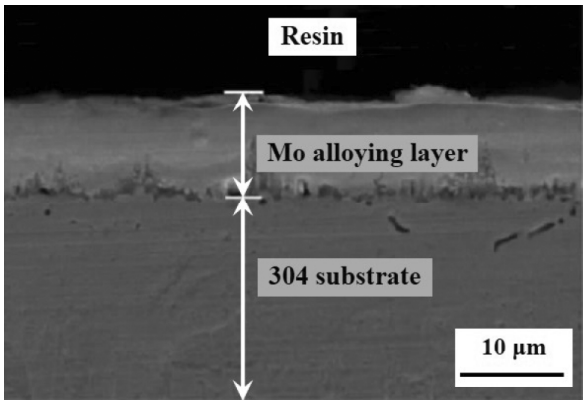

Fig. 14. Microstructure of the cross-section of Mo alloying layer. reprinted with permission from C.S. Liu, L. Qin, C.L. Li, Y. Yin, Y.B. Jia and L.L. Guo // Surf. Technol. 43 (2014) 100. (c) 2014 Surface Technology Editorial Office.

Li et al. [31] discovered a way to obtain a cermet surface layer that titanium and carbon be alloyed on the surface of 20 steel by DGPSA. The thickness of alloying layer was about 21 μm, which was mainly composed of TiC particulates forming a dense structure. The bonding strength between coating and substrate was of 42 N. The quality of coating was greatly affected by the distance between source and substrate. A good quality can be achieved with a distance of 12-16 mm. Under this condition the surface hardness was 10 times higher than the substrate.

Wang et al. [32] treated 316 stainless steel with plasma titanizing-thermal oxidation treatment to enhance the surface performance of 316L stainless steel and to meet the service requirements in medical environment. The TiO_2 film was homogeneous and dense. Both Ti and O elements showed a gradient distribution along the layer depth, and the thin film exhibits an anatase TiO_2 structure. The thin film showed the higher hydrophilicity, and the contact

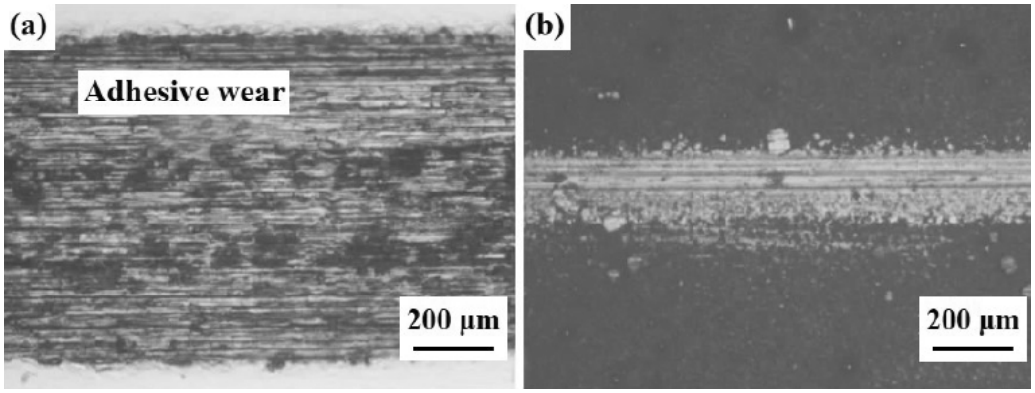

Fig. 15. Wear scar of samples after reciprocating sliding for 30 m: 304 stainless (a), Mo alloying layer (b). reprinted with permission from C.S. Liu, L. Qin, C.L. Li, Y. Yin, Y.B. Jia and L.L. Guo // Surf. Technol. 43 (2014) 100. (c) 2014 Surface Technology Editorial Office.

angle was lowered to 8.5° within 30 min under visible light irradiation condition. A ball-on-disc wear test, under the imposed load of 7.6 N, the friction coefficient of thin film with taking Al_2O_3 ceramic ball as friction pair was in the range from 0.30 to 0.40, and the wear rate was only 1.14×10^{-4} $mm^3\cdot N^{-1}\cdot m^{-1}$. The wear resistance and antifriction performance of TiO_2 film after duplex treatment were much superior to those of stainless steel substrate.

Wang et al. [33] penetrated copper and cerium on 304 stainless steel by DGPSA. With the content of cerium in source cathode increasing, the content of cerium and copper increased, the depth of diffusion layer became thicker and the depth of deposition layer got thinner. The surface hardness of diffused layer was obviously improved.

Gao et al. [34] achieved plasma chromizing on Q235 steel and 45 steel surface to form high chromium layer. Then plasma carburizing was proceed on alloyed high chromium layer. The results showed the surface chromium composition content was more than 40% and the chromium element was infinity dissolved into α-Fe. The chromium composition of alloyed layer indicated a gradient distribution. The carbonization of alloyed layer was secondly carbides from solid. The carbides were dispersion, thin and uniform. The carbon content on the surface was more than 2.8%. There was no ledeburite phase in the alloyed layer. The surface hardness in alloyed layer was 1800 HV after quenching and tempering. The wear resistant was 7 times higher than that of GCr15 steel.

Hong et al. [35] produced titanized layer on T10 steel by DGPSA. The results showed that the TiC layer formed on the sample surface was homogeneous, dense and was metallurgically combined with the substrate. The microhardness of the tetanized layer was up to 1100 $HV_{0.01}$, and gradually decreased with the depth increased. Compared with the as-received substrate, the friction coefficient of the tetanized layer was reduced and exhibited excellent anti-wear property.

Xu et al. [36] prepared Mo-Cr penetrating layer on Q235 low-carbon steel by DGPSA and then the technological process of ultra-saturated carbonization, quenching and low tempering was conducted. The depth of coating was over 100 μm. The abrasion experiment results showed that the average friction coefficient was 0.1 and the average relative wear ability was 2.25 times as much as one of GCr15.

Kui et al. [37] synthesized TiN permeation layer on the surface of Q235 steel using DGPSA, and then TiB_2 film was deposited on the surface of permeation layer by direct current magnetic reactive sputtering method to form TiN/TiB_2 multi-permeation layer. The surface appearance was very uniform, compact and fine. Surface microhardness of TiN/TiB_2 multi-permeation layer was 2600 HV averagely and the mean friction coefficient of TiN/TiB_2 multi-permeation layer was less and its grinding trace was also shallower than that of Q235 steel.

Xu et al. [38] prepared Mo-Cr alloying layer on Q235 steel by DGPSA. Strengthened layer were made on the Mo-Cr alloying layer by ultra-saturated carbonization, quenching and low tempering. The results indicated that the depth of coating was over 100 μm. After quenching + low tempering, it was found that the hardness of surface alloying was up to 1300 HV. The abrasion experiment results showed that the average friction coefficient was 0.1 and the average wear resistance was 2.25 times higher in comparison to GCr15.

Liu et al. [39] made the high chromium and carbon alloying layer on 20 steel surfaces by DGPSA and carburization. The concentrations of chromium and carbon as well as the mass percentage of carbides (more than 40%) in the alloying layer were higher than those of integral cast irons. The carbides distributed in the alloying layer were mainly $M_{23}C_6$ and M_7C_3 with a size of about 1 μm. The micro-hardness value of the alloying layer was 1000~1600 HV and the wear resistance increased 8.6 times compared with GCr15 steel.

Xu et al. [40] investigated the wear properties of the Mo-Cr low-alloy high speed steel (HSS). Mo-Cr penetrating layer on Q235 steels were formed by DGPSA and then ultra-saturated carbonization, quenching and tempering were conducted. The results indicated that the depth of coating was over 100 μm. After quenching and tempering, it was found that the hardness of surface alloying was up to 1300 HV.

Wang et al. [41] obtained N-doped TiO_2 (N-TiO_2) coatings by oxidation of titanium nitride coatings, which were firstly prepared by the DGPSA on stainless steel (SS). Ball-on-disc sliding wear was applied to test and compare the tribological behaviors of the coatings and the substrate. The results showed that anatase type TiO_2 existed in the coatings after oxidation, the obtained coatings had a layered structure, consisted of N-TiO_2 layer at the top and a diffusion-type interface. Such a hybrid coatings system showed good adhesion with the substrate. Continuous and compact coatings were observed by SEM images after oxidation. Under a load of 7.6 N, the coefficient of friction was in the range of 0.27~0.38 for the N-TiO_2/Al_2O_3 systems and the wear rate of the coatings was only 1/14 of that for untreated 316L SS. N-TiO_2 coatings displayed much better wear resistance and antifriction performance than SS substrate.

Zhang et al. [42] conducted W-Mo-Co layer on the surface of T8 steel by DGPSA. The surface alloyed layer were composed of M_6C+MC type carbide layer and solid solution layer of W, Mo, Co. Hardness of carbide layer were 1200~1400 $HV_{0.025}$. Hardness of solid solution layer were only 400~550 $HV_{0.025}$ and could be improved to 800~1000 $HV_{0.025}$ by subsequent ageing treatment. The alloyed layer also showed high bonding strength with the substrate.

Li et al. [43] formed a W-Mo-Co alloyed layer on 25Cr2Mo2V by the DGPSA. The results showed that the structure of the surface alloying layer was low-carbon martensitic with low hardness of 430 $HV_{0.2}$ after solution at 1240 °C for 5 min. The hardness of the surface alloying was increased from 430 $HV_{0.2}$ to 1130 $HV_{0.2}$ after aging treatment for 40 min at 540 °C, with precipitation of tiny intermetallic and carbides. This surface age-hardening alloyed layer also possessed good resistance against temper softening, its surface hardness still exceeded 680 $HV_{0.2}$ after tempering for 2 h at 700 °C.

Wang et al. [44] prepared W-Mo-Ti alloying by DGPSA process to form a similar high speed steel components alloying layer. The results showed that the microstructure of the alloying layer consisted of alloying ferrite, and the composition of the alloy elements was 8 wt.% W+10 wt.% Mo+1.8 wt.% Ti. After successive carburizing, the alloying layer consisted of uniform and fine granular pearlite. After quenching and tempering, the alloying layer was composed of tempered martensitic and the fine carbides were M_6C (Fe_3W_3C), M_7C_3 [$(FeWMo)_7C_3$], and MC(TiC; γ-MoC). The carbides was smaller and more uniform, the hardness of the alloying layer was 800~890 $HV_{0.1}$ and the red hardness was 760 $HV_{0.1}$.

Wu et al. [45] firstly conducted W-Mo-Y surface alloying process and W-Mo surface alloying on Q235 steels by DGPSA in order to form a uniform dense alloying-diffusion-layer. Then both obtained coatings were treated by carburizing at 960 °C, 980 °C, and 1020 °C for 8 h and then conducted quenching process. Afterwards tempering processes were carried out at 200 °C, 300 °C, 400 °C, 500 °C, 600 °C, and 700 °C, respectively, with thermal insulation for 1 h at every temperature to W-Mo-Y layer and W-Mo layer. The results showed that the tempering behavior was the same as that of metallurgy high speed steel. The secondary hardening appeared at 500 °C, and the tempering hardness peaked at 500 °C. And the hardness values of W-Mo-Y layer were higher than that of W-Mo layer. When W-Mo-Y layer and W-Mo layer were subjected to carburizing and quenching process at 1020 °C, as well as thermally insulated at 600 °C for 1 h and then followed by air cooling, their maximum hardness values were 750 $HV_{0.05}$ and 650 $HV_{0.05}$, respectively. It was seen that with the addition of Yttrium, the surface hardness, tempering hardness and red-hardness of the diffusion layer were increased.

Luo et al. [46] fabricated a Fe-Al-Cr-Nb alloyed layer onto the surface of 45 steel by DGPSA. The obtained alloyed layer with a thickness of 20 μm was homogeneous and compact. The alloyed elements exhibited a gradient distribution along the cross section. Microhardness and nanoindentation tests implied that the surface hardness of the alloyed layer reached HV 580, which was almost 2.8 times of the substrate. Compared with the substrate,

the alloyed layer had a much smaller displacement and a larger elastic modulus. According to the friction and wear tests at room temperature, the Fe-Al-Cr-Nb alloyed layer had lower friction coefficient and less wear mass, indicating that the Fe-Al-Cr-Nb alloyed layer could effectively improve the surface hardness and wear resistance of the substrate.

Liu et al. [47] prepared TiN alloy layer on the surface of steel material by DGPSA. The surface of permeating alloying layer were uniform and compact. The atom concentrations of Ti and N gradually distributed along the depth of the alloying layer. The formed TiN layer was composed of a deposition and a diffusion layer. The TiN alloying layer which reached a thickness of 8 μm had improved the wear resistance of steel indicating by a narrower wear trace.

Tang et al. [48] studied the microstructures of the plasma alloying high speed steel on 20 steel by DGPSA with Mo, W, and carburizing. The results showed that the hardness and hot hardness were equal to that of M2 steel.

Tian et al. [49] formed a G3 alloy-like coating on P110 oil casing tube steel via DGPSA to improve its surface performance and prolong its service life-time. The received G3 alloy-like coating was uniform and compact. The wear resistance of the G3 alloy-like coating was measured by reciprocating type tribometer under dry sliding against GCr15 steel and Si_3N_4 counterparts. The G3 alloy-like coating exhibited higher surface hardness value and lower mass losses than those of P110 steel. G3 alloy-like coating showed no obvious friction-reduction effect, but revealed good wear resistance by lower mass losses. G3 alloy-like coating held higher open circuit potential (OCP) and lower current density as compared with P110 steel; which presented excellent corrosion resistance in CO_2-saturated simulated oilfield brine

Li et al. [50] designed six processes about multi-element alloying sequence to alloying with N, C and Ti on the surface of 20 carbon steel by DGPSA. In the first three plans, no film had been produced. In No.4 plan, a 7 μm alloying layer which was composed of $Ti_2C_{0.06}$ and Ti_2N phases. Its surface hardness and wear resistance were 3 times and 1 time higher than the substrate, respectively. It was also found that the films with 40 μm had been produced in No.5 and No.6 plan. These films were composed of TiN and TiC phases and the adhesion with substrate exhibited well. The surface hardness of alloying layer was over 2100 HV and the wear resistance was 8 times higher than that of substrate.

3.2. Corrosion resistance

He et al. [51] prepared Cu modified layer on surface of 304 stainless steel by DGPSA and then plated Ag coating on the Cu modified layer through electroless plating. The corrosion and antibacterial properties of the modified samples were studied and analyzed. The results revealed that Ag-Cu platting layer had good corrosion resistance and high bonding strength with substrate. Compared with Cu-alloyed and untreated substrate materials, the antibacterial property was obviously improved, the sterilization rate was up to 100%.

Zhu et al. [52] synthesized a binary Fe-Al alloyed layer on 45 steel by DGPSA. The modified layer was composed of a deposition layer and a diffusion layer, with a total thickness of about 180 μm. The protective film exhibited high microhardness. The corrosion resistance for the layer in 2.0% Na_2S and 0.05 mol/L Na_2SO_4 + 0.5 mol/L NaCl mixed solutions had been increased to more than 6 times.

Zhu et al. [53] synthesized a Ni-Cr alloyed layer on Q235 steel by using DGPSA. The Ni- Cr alloyed layer was uniform, dense and without any cracks or holes. The average thickness of the alloyed layer was about 12 μm. The received alloyed layer was composed of $FeCr_{0.29}Ni_{0.16}C_{0.06}$, $Cr_{23}C_6$ compound phases and ã solid solution phase. The contents of Ni and Cr gradually decreased from the surface to the interior. The surface microhardness of the alloyed layer was 9.72 GPa. The Ni-Cr alloyed layer could improve the corrosion resistance of Q235, even better than that of 304L stainless steel.

Gao et al. [54] directly synthesized TiN coating by DGPSA on the surface of 20 steel. The formed structure was solid solution diffusing layer and TiN deposition layer. There was a metallurgical bonding between the TiN coating and the matrix. The surface hardness of infiltrating layer was 2300 HV. The electrochemical corrosion experiments were carried out on the plasma multi-infiltration TiN and Q235 steel in the 10% H_2SO_4, 5% HCl and 3.5% NaCl water solution and H_2S pregnant solution (H_2S: 5~8 g/L,$NH_3 \cdot H_2O$: 20 g/L). The results showed that the corrosion resistance of multi-infiltration samples was increased to 789, 26, 3.3, and 67 times of the Q235 steel samples.

Liu et al. [55] formed TiN multi-permeated layers with diffusion layer and deposition layer on the steel surface by means of both DGPSA and reactive sputtering. The TiN multi-permeated layer was uniform and compact, the atomic contents of Ti, N gradually decreased with increasing distance from

the surface. The adhesion of the TiN coating was very strong, its thickness was more than 10 μm.The corrosion resistance of the TiN multi-permeated layer in 10% H_2SO_4 and 3.5% NaCl were promising, the corrosion rate were only 0.156 g/(m^2·h) and 0.025 g/(m^2·h), respectively.

In order to improve the corrosion resistance of Q235 steel, Ruan et al. [56] applied DGPSA steel to prepare Ni-Cr alloyed layer on the surface of Q235 steel. With increasing the electrode distance, the thickness of Ni-Cr alloyed layer showed trend of firstly increased and then decreased. The Ni-Cr alloyed layer was dense, and had a metallurgical bonding with substrate. The thickness of Ni-Cr alloyed layer was 95 μm, and the main phase of alloyed layer was $Ni_{2.9}Cr_{0.7}Fe_{0.36}$ and minor Ni_3Fe. The polarization curve indicated that the Ni-Cr alloyed layer showed more difficult electrochemical corrosion reaction and lower corrosion rate. The results demonstrated that the corrosion resistance of Q235 steel was significantly improved after surface Ni-Cr alloying.

In order to obtain a high-performance surface on stainless steel of coal mine machine, Li et al. [57] prepared Ti-N modified layer on surface of stainless steel with DGPSA. Electrochemical analysis techniques were employed to measure the corrosion resistance of stainless steel substrate and the Ti-N coating. The results revealed that Ti-N coating exhibited lower current density and corrosion rate in comparison to the stainless steel substrate. Ti-N modified layer has significantly improved corrosion resistance of stainless steel.

Bu et al. [58] carried out plasma titanizing + plasma nitridizing on the surface of carbon steel. Corrosion experiment of treated sample in 1 mol/L HNO_3 solution was carried out using electrochemical tests. The results showed that the corrosion resistance of TiN layer and Ti alloy layer were enhanced by 4.54 times and 7.44 times. The corrosion mechanisms of untreated carbon steel, Ti alloy layer and TiN layer were pitting, light aspect corrosion and intergranular corrosion, respectively.

Fan et al. [59] obtained Ni-Cr surface metallizing for A3 steel sheet by DGPSA. The thickness of the Ni-Cr diffusion layer varied form several ìm up to 300 μm. The concentrations of Ni and Cr were up to 80% and the rust resistance was better than stainless steel. Now the steel plate with a size of 1000 mm × 500 mm could be treated with this process. The successful research of this technology provided a new way to replace part of stainless steel by carbon steel, which had both high technical value and economic benefit.

Yuan et al. [60] treated the 201 stainless steel through the strengthening treatment with both DGPSA nitriding and multi-arcion plating TiN to improve its corrosion resistance. The results showed that the outer layer of the composite strengthened layer was a compact TiN layer with a thickness of 1.2 μm, the middle layer was a nitrided layer with a thickness of 20 μm. The main phases in composite strengthened layer contained TiN, Ti, CrN, Ni_3N, Fe_3N, Fe_7C_3. Polarization curves of the composite strengthened layer and 201 stainless steel in 3.5% NaCl, 1mol/L NaOH and 1mol/L H_2SO_4 solution were measured by electrochemical tests. The corrosion resistance of composite strengthened layer was nearly the same as that of 201 stainless steel in 3.5% NaCl solution, but increased 7 times in 1 mol/L NaOH solution and 14 times in 1 mol /L H_2SO_4 solution.

Zhou et al. [61] obtained Nb alloyed layer on Q235 steel by DGPSA. The modified layer was a duplex layer (deposited + diffused layer) with a thickness of about 25 μm, which was composed of Nb, Fe_2Nb and NbC. The coating was metallurgically bonded to the substrate. In 5% H_2SO_4 solution, the corrosion rate of Nb alloy diffusion layer and the substrate were 0.649 g/(m^2·h), 6.695 g/(m^2·h), which meant that the corrosion resistance of Q235 steel was significantly improved.

Xie et al. [62] employed DGPSA to synthesis Nb-alloying, the obtained coating significantly improved the resistance to intergranular corrosion. A continuous and compact Nb modified surface alloying layer was obtained on 0Cr18Ni9 austenitic stainless steel substrate and the thickness was about 22 μm (Fig. 16). Intergranular corrosion test results showed that the untreated 0Cr18Ni9 stainless steel showed three kinds of gully intergranular corrosion, while almost no intergranular corrosion took place on the Nb alloying layer. The NbC and Nb_6C5 formed within the Nb alloyed layer reduced the precipitation of $Cr_{23}C_6$, and then enhanced the intergranular corrosion resistance.

Cheng et al. [63] conducted chromizing on 3Cr13 stainless steel at 700 °C, a decarburizing layer formed under the chromizing coating with depth of 4~5 μm. Surface hardness of the sample reached 728 $HV_{0.05}$, the major phases of the coating were Fe, Cr, $Cr_{1.36}Fe_{0.52}$ and $Cr_{23}C_6$; the corrosion resistance for the layer in 2.5% HCl solution was increased to more than 6 times. In respect of 3Cr13 stainless steel, its resistance to pitting corrosion increased to a certain degree, and its anti-intergranular corrosion property was also improved after DGPSA chromizing.

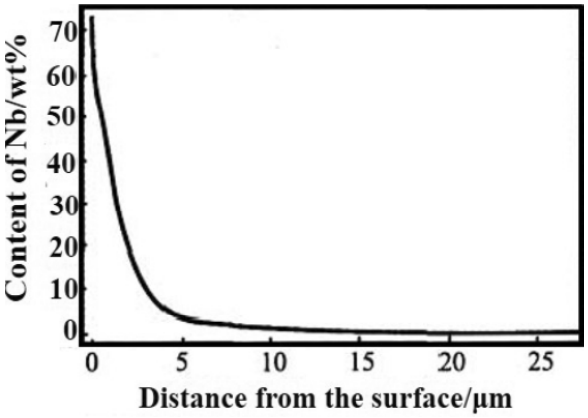

Fig. 16. The depth changing of the niobium modified layer. reprinted with permission from Y.X. Xie, J. Liu, Z.X. Wang and Z.Y. He // Hot Working Technol. 38 (2009) 71. (c) 2009 Hot Working Technology Editorial Office.

Liu et al. [64] achieved Ti alloying on the surface of 316L stainless steel by using DGPSA to improve the intergranular corrosion resistance. The modified alloy layer that formed in the condition of 1000 ! for 3.5 h consisted of TiC and Ti_8C_6. In the 10% oxalate etching tests, 316L stainless steel appeared intergranular corrosion of concave organization; there was no intergranular corrosion in Ti alloy layer. The Ti alloying treatment had notably improved the intergranular corrosion resistance of 316L stainless steel.

Xu et al. [65] produced a high chromium alloyed layer on Q235 steel with DGPSA. The Cr content of alloyed layer was about 40% on the surface of Q235 steel and the depth of coating was about 50 μm. Then an ultra-saturation carbonization treatment was followed to realize the surface carbon content reaching around 2.7%. After quenching and low-tempering heat treatment, the carbides were $M_{23}C_6$ and M_7C_3 in the layer. In 10% H_2SO_4, 3.5% NaCl water solutions and H_2S pregnant solution (H_2S 5~8 g/L + $NH_3 \cdot H_2O$ 20 g/L), the electrochemical corrosion experiments were carried out on the Cr coated samples and Q235 steel sample respectively. The results indicated that the corrosion resistance of the double glow plasma chromized samples was increased 2.35, 3.10, and 2.14 times regarding to Q235 steel samples.

Xu et al. [66] studied the multi-element Ni-Cr-Mo-Cu surface alloying layer on the substrates of 20 low carbon steel and Cr18Ni9 stainless steel by means of DGPSA. The corrosion resistance of the alloying layer was investigated by electrochemical tests in 5% HCl solution. The results showed that the chemical composition of surface alloying layers formed on the substrates were similar to Hastelloy C-2000 alloy. The corrosion resistance of alloyed layer formed on the stainless steel was close to the one of Hastelloy C-2000 alloy and better than the alloy 59. The corrosion resistance of alloyed layer formed on the low carbon steel was better than that of Cr18Ni9 stainless steel. Furthermore, Xu et al. [67] also investigated the corrosion resistance of the composite of Ni-Cr-Mo-Cu multi-element surface alloying with electric brush plating Ni interlayer on the low carbon steel substrate in 5% HCl solution. The results indicated that the corrosion resistance of the new type composite alloyed layer was better than that of single Ni-Cr-Mo-Cu multi-element surface alloying or electric brush plating layer.

Lu et al. [68] prepared a zirconium modified alloying layer on 0Cr18Ni9Ti stainless steel by DGPSA to improve its corrosion resistance in acid environment. Alloying elements in the Zr-alloyed layer presented gradient distribution and a dense zirconium oxide passivation film was formed on its surface, so acid corrosion resistance of Zr-alloyed layer was significantly improved as compared with the stainless steel substrate. The electrochemical corrosion tests of stainless steel substrate and Zr-alloyed layer samples were conducted in 0.5 mol/L H_2SO_4. The results showed that the corrosion rate of stainless steel sample was 2.18 times of the Zr-alloyed layer in H_2SO_4 solution. Surface corrosion of stainless steel samples more serious, however only minor localized corrosion pitting was observed on the surface of Zr-alloyed layer.

Wang et al. [69] studied the microstructure, composition and corrosion resistance of Ta modified layer on low carbon steel Q235 obtained by DGPSA. The results showed that the tantalum element distributed gradually from the surface to substrate. Ta modified layer was well bonded to the substrate. The corrosion resistance of Ta modified layer was better than that of the substrate, and its protection efficiency was 99.88%.The passive film on Ta modified layer was integral and could effectively protect the substrate.

Cai et al. [70] prepared a continuous and compact zirconium modified surface alloying layer on 0Cr18Ni9Ti austenite stainless steel substrate by DGPSA. The phases of Zr-alloyed layer were mainly $ZrFe_2$, ZrC. The relative corrosion rates of stainless steel were 24.43, 2.44 and 1.90 times of Zr-alloyed layer in 0.5 $mol \cdot L^{-1}$ HCl solution, 3.5% NaCl solution and 0.5 $mol \cdot L^{-1}$ NaOH solution, respectively. The surface of unprocessed stainless steels received serious corrosion, however the surface of Zr-alloyed layers only existed slight local corrosion.

Lin et al. [71] conducted DGPSA to form a layer on 316L stainless steel substrate, which was Al layer with α-Al_2O_3 seed crystals and the rare earth element Y. And then oxidized at 580 °C. The results indicated that the coatings were dense and uniform. Element of Y was discontinuously distributed, which was mainly concentrated at the grain boundary of the coating. After plasma oxidation, Y was oxidized to Y_2O_3. The Al-Y oxide coatings contained large amounts of α-Al_2O_3 crystals. The increase of the Y content improved the bonding strength of the coatings. The corrosion current of the oxide coatings was reduced by three orders of magnitude.

Cai et al. [72] investigated the high temperature oxidation resistance of OCr18Ni9Ti stainless steel after DGPSA zirconizing treatment. After oxidizing in static air at 1150 °C for 20 h, the ratios of oxidation mass gains of the samples after zirconizing process to oxidation mass gains of untreated substrate was just 0.12, which indicated that its oxidation resistance was significantly improved.

Luo et al. [73] employed DGPSA to prepare Fe-Al-Cr alloyed layers onto the surface of low carbon steel Q235. Isothermal oxidation tests were carried out to analyze their high temperature oxidation behavior. The structure of the Fe-Al-Cr alloyed layer was compact without any microstructure defects. The as-received alloyed layers were tested under air atmosphere at different temperatures of 500 °C, 600 °C and 700 °C. At the high temperature of 700 °C, a new compact Al_2O_3 protective film occurred on the surface of the alloyed layer, replacing the destroyed Cr_2O_3 film. This Al_2O_3 film will continue to prevent the further oxidation corrosion of the alloyed layer. At the temperatures of 500 °C and 600 °C, the high temperature oxidation resistance of the Fe-Al-Cr alloyed layer was similar to that of the 304 steel, but 2~3 times higher than that of the Q235 steel. While at 700 °C the Fe-Al-Cr alloyed layer exhibited much better oxidation resistance than that of the 304 steel (2.5 times) and the Q235 steel (5.5 times).

Ni et al. [74] obtained Ag-Cu layer on AISI304 stainless steel by DGPSA. The weight ratio of silver and copper ions existed in the doped layer was 4.9:3. The corrosion potential of the layer increased from -0.103 V to 0.07 V. The corrosion current densities decreased from $1.66\times10^{-7}A/cm^2$ to $5.813\times10^{-9}A/cm^2$. The corrosion resistance of stainless steel was enhanced after doped with copper and silver ions. And Ag-Cu layer doped on stainless steel had excellent antibacterial activities (100%) against both Gram-negative Escherichia coli and Gram-positive Staphylococcus aureus.

3.3. Antibacterial and photocatalysis property

Ni et al. [75] employed DGPSA to synthesis Cu-Zn coating on AISI304 stainless steel. The results showed that the Cu/Zn co-permeated coating had a thickness of about 4 μm and was mainly composed of Cu-Zn alloy. The Cu/Zn co-permeated coating was able to kill both Escherichia coli and staphylococcus aureus by a rate of 100%. Besides, Cu/Zn doped stainless steel possessed much better corrosion resistance than the un-doped stainless steel.

Wang et al. [76] prepared antibacterial stainless layer with silver by DGPSA. The process parameters were available as follows: voltage 1.2 kV, gas flow 20~40 ml/min, 800~950 °C, soaking time 3 h. Ag existed in monovalent ion state in the modified layer, so that the surface had antibacterial ability. The antibacterial rate was 100%, and the corrosion resistance was not weakened.

Wang et al. [77] employed DGPSA combined with the copper hollow cathode effect to synthesis Cu-Ce coating on 304 stainless steel. Antibacterial experiments showed that 304 stainless steel after infiltration had good antibacterial property to E.coli and S.aureus.

In order to obtain a high-performance surface on 316L stainless steel (SS) that could meet the requirements in medical material environment, Wang et al. [78] synthesized nitrogen-doped titanium dioxide ($TiO_{2-x}N_x$) by oxidative annealing the resulted TiN_x coatings in air that were deposited by DGPSA. Such a hybrid structured coatings system was found to possess good adhesion strength with the substrate. The bacterial adherence tests demonstrated that the N-doped TiO_2 coatings could inhibit the Streptococcus Mutans adherence compared with SS substrate. The photocatalysis and positive adhesion free energy of the N-doped TiO_2 coatings affected the bacterial attachment characteristics.

4. SUMMARY

Iron and steel materials are widely used in construction and other applications because of its high tensile strength and low cost. Evidence showed that the composition and hardness of material surface play an important role in its corrosion and wear resistance. According to the literature, the improved surface performance of iron and steel materials can be achieved by DGPSA due to surface hardness and surface composition be changed. Meanwhile, the obtained alloying coatings have a strong metallurgical bond with the substrates. The positive roles in wear and corrosion behaviors of the selected al-

loying elements in alloyed coatings lie in the following aspects: 1) Formations of hard/friction-reduction phases in the coatings or in the near surfaces of iron and steel materials and receiving hard/friction-reduction surfaces by obtaining intermetallic compounds, solid solution or dispersion strengthening on the near-surfaces; 2) The obtained alloyed coatings are easy to passive, and also can play a barrier or reduce oxygen diffusion effects and form a protective dense oxide scale with high bond strength with the substrate; 3) Functions or/and effects of some metallic elements can be endowed to iron and steel materials via DGPSA.

As the special structure of nano-material is able to bring about excellent properties, nanocrystallization technology + DGPSA might be considered to improve the surface performance of iron and steel materials. Combining DGPSA with other surface technologies, duplex treatments of surface texturing + DGPSA and spraying/deposition + DGPSA might also be effective to enhance the surface protection on iron and steel materials.

ACKNOWLEDGEMENT

This work was supported by the National Natural Science Foundation of China (No.51501125 and No. 51474154), the China Postdoctoral Science Foundation (No.2012M520604 and No. 2016M591415), the Natural Science Foundation for Young Scientists of Shanxi Province (No.2013021013-2 and No.2014011015-7),), the Youth Foundation of Taiyuan University of Technology (No.2012L050 and No.2013T011), the Qualified Personnel Foundation of Taiyuan University of Technology (No. tyutrc201157a).

REFERENCES

[1] S.W. Yu, K. You, X.Z. Liu, Y.H. Zhang, Z.X. Wang and X.P. Liu // *Surf. Rev. Lett.* **23** (2016) 1650017-1.

[2] N.M. Lin, R.Z. Xie, P. Zhou, J.J. Zou, Y. Ma, Z.X. Wang, P.J. Han, Z.H. Wang, B. Tang and W. Tian // *Surf. Rev. Lett.* **23** (2016) 1630002-1.

[3] M. Łępicka and M. Grądzka-Dahlke // *Rev. Adv. Mater. Sci.* **46** (2016) 86.

[4] N.M. Lin, H.Y. Zhang, J.J. Zou and B. Tang // *Rev. Adv. Mater. Sci.* **38** (2014) 61.

[5] J. Xu, X. Zhang, X.S. Xie, Z. Xu and W.J. Liu // *Vacuum* **72** (2004) 489.

[6] Z. Xu, L. Qin, B. Tang, Z.Y. He, X.S. Xie and C.L. Zheng // *Acta Metall. Sin. Eng. Lett.* **15** (2002) 172.

[7] N.M. Lin, J.J. Zou, M.L. Li, J.W. Guo, Y. Ma, Z.X. Wang, Z.H. Wang, X.P. Liu and B. Tang // *Rev. Adv. Mater. Sci.* **44** (2016) 238.

[8] Z.Y. He, Y. Gao, F.Y. Gu, Z. Xu and J.X. Zhao // *Hot Working Technol.* **2** (1994) 8.

[9] C.Z. Wang, Y.A. Su, B. Tang and Z. Xu // *Hot Working Technol.* **2** (1994) 29.

[10] B. Tang, Y.A. Su, C.Z. Wang and Z. Xu // *Hot Working Technol.* **1** (1993) 21.

[11] X. Zhang, T.H. Zhang, X.S. Xie, J.X. Dong, Z.M. Yang and Z. Xu // *J. Beijing Norm. Univer. Nat. Sci.* **36** (2000) 757.

[12] B. Zhao, J.S. Wu, Z.H. Li, X.P. Liu, Y. Gao and Z. Xu // *The Chin. J. Nonferr. Met.* **10** (2000) 676.

[13] X.D. Gu, Z.J. Yao, X.L. Zhu, P.Z. Zhang and Z. Xu // *Heat Treat. Met.* **33** (2008) 61.

[14] G.T. Bu, Y. Gao and C.L. Wang // *Rare Met. Mater. Eng.* **39** (2010) 357.

[15] C.Z. Wang, Y.A. Su, B. Tang and Z. Xu // *Hot Working Technol.* **4** (1995) 7.

[16] Z.L. Li, J. Tao, H.B. Liu, Q. Gao, J. Xu and X.Y. Luo // *Atom. Energy Sci. Technol.* **42** (2008) 217.

[17] N.J. Ren, W.Q. Wang, Y.M. Zhang, Z.H. Li and Z. Xu // *J. Taiyuan Univer. Technol.* **34** (2003) 261.

[18] C.L. Wang, Y. Gao, G.T. Bu and G. Shen // *Surf. Technol.* **39** (2010) 47.

[19] P. Zhou, Q. Miao, P.Z. Zhang and Z. Xu // *J. Iron Steel Res.* **21** (2009) 56.

[20] Z.K. Qiu, P.Z. Zhang, D.B. Wei, X.F. Wei and X.H. Chen // *Surf. Coat. Technol.* **278** (2015) 92.

[21] X.Y. Zhang, B. Tang, A.L. Fan, Y. Ma and L.H. Tian// *J. Wuhan Univer. Technol. Mater. Sci. Ed.* **27** (2012) 260.

[22] X.Y. Zhang, B. Tang, A.L. Fan, R.H. Zhu and H.F. Wang // *Trans. Mater. Heat Treat.* **32** (2011) 136.

[23] Y. Gao, J.Y. Xu, Q. Gao, J.P. An and Z. Xu // *Tool Eng.* **40** (2006) 30.

[24] H.H. Shen, L. Liu, X.Z. Liu, Q. Guo, T.X. Meng, Z.X. Wang, H.J. Yang and X.P. Liu // *Appl. Surf. Sci.* **388** (2016) 126.

[25] H.Y. Wu, H.Y. Wei, H. Ghulam, K.M. Tao, I. Asif and W.F. Rao // *J. Wuhan Univer. Technol. Mater. Sci. Ed.* **31** (2016) 422.

[26] N.M. Lin, P. Zhou, H.W. Zhou, J.W. Guo, J.J. Zou, W. Tian, X.F. Yao and B. Tang // *Kovove Mater.* **53** (2015) 147.

[27] Y. Zheng and Y. Gao // *Mater. Heat Treat.* **36** (2007) 57.

[28] C.Z. Chi, Y. Gao, J.X. Zhao and Z. Xu // *J. Taiyuan Univer. Technol.* **34** (2003) 285.
[29] C.S. Liu, L. Qin, C.L. Li, Y. Yin, Y.B. Jia and L.L. Guo // *Surf. Technol.* **43** (2014) 100.
[30] H.B. Liu, T. Jie, J. Xu, Z.F. Chen and X.Y. Luo // *Appl. Surf. Sci.* **256** (2010) 5939.
[31] L.P. Li, Z.J. Yao, X.L. Zhu, Q. Miu, P.Z. Zhang and Z. Xu // *J. Southeast Univer. Nat. Sci. Ed.* **37** (2007) 980.
[32] H.F. Wang, X.F. Shu, X.Y. Li and B. Tang // *J. Shenyang Univer. Technol.* **35** (2013) 41.
[33] Y. Wang, J.Y. Xu, C. Gao, B. Gao and Y.M. Li // *Ordnance Mater. Sci. Eng.* **35** (2012) 9.
[34] Y. Gao, J.Y. Xu, Q. Gao, J. Cheng and Z. Xu // *Mater. Mech. Eng.* **30** (2006) 25.
[35] X.L. Hong, X. Wang, J.Y. Yang, C.C. Ji and X.C. Wei // *China Surf. Eng.* **26** (2013) 49.
[36] J.Y. Xu, Y.M. Song, Y. Gao, Y.J. Yu and Z. Xu // Acta Arma. **27** (2006) 1068.
[37] X.Y. Kui, J.Z. Wang, Y.P. Liu, J.Y. Xu, Y. Gao and Z. Xu // *Trans. Nonferr. Met. Soc. China* **15** (2005) 411.
[38] J.Y. Xu, Y. Gao, Y.M. Song, Q. Gao and Z. Xu // *Mater. Eng.* **51** (2006) 239.
[39] X.P. Liu, Y. Gao, J.Y. Xu, Y.P. Liu, J.Z. Wang, X.Y. Kui and Z. Xu // *Mater. Sci. Technol.* **14** (2006) 251.
[40] J.Y. Xu, L. Du, Y.P. Liu, J.Z. Wang, X.Y. Kui, Y. Gao and Z. Xu // *Mater. Sci. Technol.* **14** (2006) 412.
[41] H.F. Wang, B. Tang and X.Y. Li // *J. Iron Steel Res., Int.* **18** (2011) 73.
[42] Y.M. Zhang, Z.H. Li, P.Z. Zhang and Z. Xu // *J. Taiyuan Univer. Technol.* **37** (2006) 427.
[43] Z.H. Li, N.J. Ren, Y.M. Zhang and Z. Xu // *Ordnance Mater.Sci. Eng.* **27** (2004) 1.
[44] C.Z. Wang, X.K. Su, J. Ma, L.B. Zhang and Q. Liu // *Heat Treat. Met.* **29** (2004) 18.
[45] H.G. WU, H.W. Cai, Z.K. Ma, C.L. Wang, B. Li and Y. Gao // *China Surf. Eng.* **25** (2012) 1.
[46] X.X. Luo, Z.J. Yao, P.Z. Zhang, Y. Chen, H.Q. Yang, X.F. Wu, Z.L. Zhang, Y.H. Lin and S.J. Xu // *Trans. Nonferr. Met. Soc. China* **25** (2015) 3694.
[47] Y.P. Liu, J.Y. Xu, Y. Gao and Z. Xu // *China Mech. Eng.* **17** (2006) 1748.
[48] B. Tang, Y.A. Su, C.Z. Wang and Z. Xu // *Hot Working Technol.* **5** (1993) 32.
[49] W. Tian, W. Yu, N. Lin, J. Zou, J. Guo, H. Zhang, P. Zhou, R. Xie, Y. Ma and Z. Wang // *Int. J. Electrochem. Sci.* **10** (2015).
[50] L.P. Li, Z.J. Yao, K. Yan, P.Z. Zhang and Z. Xu // *J. Mater. Sci. Eng.* **26** (2008) 411.
[51] Y.H. He, J. Liu, Z.Y. He and Z.X. Wang // *Mater. Heat Treat.* **39** (2010) 179.
[52] X.L. Zhu, Z.J. Yao, X.D. Gu, W. Cong and P.Z. Zhang // *Trans. Nonferr. Met. Soc. China* **19** (2009) 143.
[53] X.L. Zhu, Z.J. Yao, W.J. Bao, P.Z. Zhang, Q. Miao and H.F. Ding // *J. Nanjing Univer. - Nat. Sci.* **45** (2009) 223.
[54] Y. Gao and Z. Xu // *New Technol. New Process* **28** (2006) 25.
[55] Y.P. Liu, J.Y. Xu, X.Y. Kui, J.Z. Wang, Y. Gao and Z. Xu // *J. Chinese Soc. Corro. Prot.* **26** (2006) 227.
[56] Y. Ruan, Y. Yin, J.Y. Kong, M. Yang, Y.J. Xiong and J. Huang // *Heat Treat. Technol. Equipt.* **36** (2015) 12.
[57] J.H. Li, J. Liu and F. Gao // *Coal Mine Mach.* **33** (2012) 58.
[58] G.T. Bu, Y. Gao, C.L. Wang and G. Shen // *Mater. Heat Treat.* **39** (2010) 127.
[59] B.H. Fan, Z. Xu, W.N. Zheng and Q. He // *Heat Treat. Met.* (1988) 37.
[60] L. Yuan, Y. Gao, W. Zhang, C.L. Wang and C.X. Huang // *Trans. Mater. Heat Treat.* **32** (2011) 144.
[61] P. Zhou, Q. Miao, P.Z. Zhang and Z. Xu // *Jiangsu Aviat.* **28** (2008) 149.
[62] Y.X. Xie, J. Liu, Z.X. Wang and Z.Y. He // *Hot Working Technol.* **38** (2009) 71.
[63] D. Cheng, Y. Gao and G.H. Tang // *Heat Treat. Met.* **34** (2009) 58.
[64] W.Y. Liu, H.F. Wang and X.Y. Li // *Sci. Technol. Innov. Prod.* **17** (2010) 99.
[65] J.Y. Xu, L. Du, X.Q. Long, W.X. Tang, Y. Gao and Z. Xu // *Corros. Sci. Prot. Technol.* **18** (2006) 306.
[66] J. Xu, X.S. Xie and Z. Xu // *Trans. Mater. Heat Treat.* **23** (2002) 28.
[67] J. Xu, X.S. Xie, Z. Xu, S.Y. Dong and B.S. Xu // *Acta Metall. Sin.* **38** (2002) 1074.
[68] X.H. Lu, Y. Gao, W.Z. Wei, G.Y. Zhang and H.W. Cai // *J. Guilin Univer. Electron. Technol.* **34** (2014) 168.
[69] R.N. Wang, P.Z. Zhang, Q. Bi, D.B. Wei and X.H. Chen // *Mate. Mech. Eng.* **37** (2013) 25.
[70] H.W. Cai, Y. Gao, Z.K. Ma and C.L. Wang // *Chin. J. Rare Met.* **37** (2013) 915.
[71] Y.B. Lin, Y.F. Zhu and W.G. Zhu // *Sci. Eng. Compos. Mater.* **24** (2017) 309.
[72] H.W. Cai, Y. Gao, Z.K. Ma and C.L. Wang // *Mater. Rev. B* **28** (2014) 97.

[73] X.X. Luo, Z.J. Yao, P.Z. Zhang, Q. Miao, W.P. Liang, D.B. Wei and Y. Chen // *Appl. Surf. Sci.* **305** (2014) 259.
[74] H.W. Ni, W.T. Zhang and R.S. Chen // *Mater. Rev. B* **25** (2011) 27.
[75] H.W. Ni, W.T. Zhang and R.S. Chen // *Mater. Prot.* **44** (2011) 25.
[76] L. Wang, Z.W. Qin, H.W. Ni, P.Y. Xiong, B.F. Xu and J. Wang // *Surf. Technol.* **35** (2006) 39.
[77] Y. Wang, J.Y. Xu, C. Gao, F. Tang and J.C. Zhao // *Rare Met. Mater. Eng.* **42** (2013) 1254.
[78] H.F. Wang, B. Tang, N.M. Lin, X.Y. Li, A.L. Fan and X.F. Shu // *J. Wuhan Univer. Technol. Mater. Sci. Ed.* **27** (2012) 542.